NASA-CR-201067

RIACS

Research Institute for Advanced Computer Science
NASA Ames Research Center

Aerodynamic design optimization via reduced Hessian SQP with solution refining

Dan Feng and Thomas H. Pulliam

RIACS Technical Report 95.24 December 1995

Aerodynamic design optimization via reduced Hessian SQP with solution refining

Dan Feng and Thomas H. Pulliam

The Research Institute for Advanced Computer Science is operated by Universities Space Research Association, The American City Building, Suite 212, Columbia, MD 21044 (410)730-2656

Work reported herein was supported in part by NASA under contract NAS 2-13721 between NASA and the Universities Space Research Association (USRA).

AERODYNAMIC DESIGN OPTIMIZATION VIA REDUCED HESSIAN SQP WITH SOLUTION REFINING*

by

Dan Feng† *and Thomas H. Pulliam*‡

*Work reported herein was supported by NASA under contract NAS 2-13721 between NASA and the Universities Space Research Association (USRA).

†Research Institute for Advanced Computer Science (RIACS), Mail Stop T20G-5, NASA Ames Research Center, Moffett Field, CA 94035-1000, USA. Phone: 415-6046362. Email: feng@riacs.edu

‡Fluid Dynamics Division, Mail Stop T27B-1, NASA Ames Research Center, Moffett Field, CA 94035-1000, USA. Phone: 415-6046417. Email: pulliam@nas.nasa.gov

Abstract

An all-at-once reduced Hessian Successive Quadratic Programming (SQP) scheme has been shown to be efficient for solving aerodynamic design optimization problems with a moderate number of design variables [1]. This paper extends this scheme to allow solution refining. In particular, we introduce a reduced Hessian refining technique that is critical for making a smooth transition of the Hessian information from coarse grids to fine grids. Test results on a nozzle design using quasi-one-dimensional Euler equations show that through solution refining the efficiency and the robustness of the all-at-once reduced Hessian SQP scheme are significantly improved.

Key words. design optimization, constrained optimization, reduced Hessian methods, quasi-Newton methods, successive quadratic programming, solution refining

Abbreviated title. Reduced Hessian SQP with solution refining

1 Introduction

An aerodynamic design optimization problem can often be posed as

$$\begin{aligned} &\min \ \ I(X,u) \\ &\text{s.t.} \ \ F(X,u) = 0, \end{aligned} \tag{1.1}$$

where $X \in \Re^n$ denotes the discretized flow variables, and $u \in \Re^m$ denotes the design variables, which, for example, could be geometry parameters describing the shape of a profile; $I : \Re^{n+m} \to \Re$ is a cost function, which may, for example, measure the deviation from a desired surface pressure distribution; $F : \Re^{n+m} \to \Re^n$ is a discretized version of the governing equations of the flow field. It is often the case that I and F are nonlinear, and the number of flow variables is much larger than the number of design variables ($n >> m$).

In [1], a reduced Hessian SQP scheme is introduced for solving (1.1). This approach treats X and u as independent variables and updates them simultaneously at each iteration. One interesting property is that the flow equations are not required to be satisfied until convergence. It is intended to alleviate the cost of repeatedly solving the nonlinear flow equations required by other methods [9, 6]. Test results show that this scheme has a potential to be very efficient. This paper shows that the efficiency of the reduced Hessian SQP scheme can be further improved through solution refining.

Solution refining techniques have been successfully used for aerodynamic design optimization by many authors [11, 7]. The basic idea is to solve the design problem on a coarse grid first, then use the coarse grid solution as an initial guess for a finer grid, and repeat this process until a solution on a desired grid is reached. Solution refining can be used with reduced Hessian SQP schemes as well. However in addition to refining solutions of flow and design variables it also needs to refine the reduced Hessian matrix approximation. This refinement is critical since the amount of Hessian information retained greatly influences the speed of convergence. However, as we are aware of, this issue has not been studied for aerodynamic design optimization. It is tempting to use the reduced Hessian approximation from the coarse grid solution directly as the initial guess for the next grid. However, this

practice may result in a mismatch of Hessian information between the two grids, particularly when unorthogonal bases are used for the null space, due to the dramatic change of bases in the null space caused by the change of grid sizes.

This paper introduces a technique that satisfactorily solves the information mismatch problem. The basic idea is to use the fact that the reduced Hessian matrix can be treated as an invariant when the basis for the null space is properly chosen. This invariant bridges the information transition of the Hessian information between two grids.

2 A review of an all-at-once reduced Hessian SQP scheme for aerodynamic design optimization

Reduced Hessian SQP is a special case of SQP, which is a mature and successful technique for solving nonlinear constrained optimization problems due to its relatively low computational cost and fast convergence.

In the context of aerodynamic design optimization problem (1.1), at each iteration of SQP, a quadratic approximation to the Lagrangian function of (1.1)

$$L(X,u,\lambda) = I(X,u) + \lambda^T F(X,u),$$

is minimized subject to a linearization of the flow equations. This gives a subproblem

$$\min_{d\in\Re^{n+m}} g_k^T d + \tfrac{1}{2} d^T H_k d \tag{2.1}$$

$$\text{subject to } F_k + A_k^T d = 0, \tag{2.2}$$

where $d = \begin{pmatrix} \Delta X \\ \Delta u \end{pmatrix}$, $g_k = \begin{pmatrix} \frac{\partial I}{\partial X} \\ \frac{\partial I}{\partial u} \end{pmatrix}$ at (X_k, u_k), $A_k = \begin{pmatrix} \frac{\partial F}{\partial X} \\ \frac{\partial F}{\partial u} \end{pmatrix}$ at (X_k, u_k), $F_k = F(X_k, u_k)$, and H_k is the Hessian (or approximation) of the Lagrangian function.

One way of solving (2.1-2.2) is via separation of variables. Suppose we can compute two matrices $Y_k \in \Re^{(n+m)\times n}$ and $Z_k \in \Re^{(n+m)\times m}$ such that the matrix $[Y_k \;\; Z_k]$ is nonsingular and $Z_k^T A_k = 0$ (Z_k is a basis for the null space of A_k^T). Let $d = Y_k d_1 + Z_k d_2$ and plug this into (2.1-2.2). If we assume $Z_k^T H_k Z_k$ is positive definite (which is reasonable because this matrix is indeed positive definite close to the solution due to the second order sufficient optimality condition), by standard techniques, d_1 and d_2 are given by

$$\begin{aligned} d_1 &= -(A_k^T Y_k)^{-1} F_k \\ d_2 &= -(Z_k^T H_k Z_k)^{-1}(Z_k^T g_k + Z_k^T H_k Y_k d_1). \end{aligned} \tag{2.3}$$

To avoid the computation of H_k, the "cross" term $Z_k^T H_k Y_k d_1$ is simply ignored and $Z_k^T H_k Z_k$ is approximated by an $m \times m$ matrix B_k using a variable metric formula such as BFGS, giving,

$$d_2 = -B_k^{-1} Z_k^T g_k. \tag{2.4}$$

Methods based on (2.3-2.4) are referred to as reduced Hessian SQP methods.

To avoid undue computational cost of orthogonal basis, many authors [3, 4, 2, 10] choose to use

$$Z_k = \begin{pmatrix} -(\frac{\partial F}{\partial X})^{-T}(\frac{\partial F}{\partial u})^T \\ I \end{pmatrix} = \begin{pmatrix} -S \\ I \end{pmatrix}, \tag{2.5}$$

where, in aerodynamic design optimization, S is the sensitivity matrix.

As analyzed in [1], the popular choice of $Y_k = [I\ 0]^T$ potentially has an undesirable effect of producing a larger cross term. Instead

$$Y_k = \begin{pmatrix} I \\ S^T \end{pmatrix}, \tag{2.6}$$

is chosen, which is likely to produce a smaller cross term. Clearly $Z_k^T Y_k = 0$ holds.

From (2.3), d_1 satisfies $(A_k^T Y_k)d_1 = -F_k$, which is equivalent to

$$\left[\left(\frac{\partial F}{\partial X}\right)^T + \left(\frac{\partial F}{\partial u}\right)^T S^T\right] d_1 = -F_k,$$

which in turn is equivalent to

$$J_k(I + SS^T)d_1 = -F_k, \tag{2.7}$$

where $J_k = \left(\frac{\partial F}{\partial X}\right)^T$ at (X_k, u_k) is the current Jacobian matrix of the flow equation. (2.7) can be solved by first solving $J_k y = -F_k$ for y, and then solving $(I + SS^T)d_1 = y$ for d_1. The solution of the former is a linear flow calculation. The solution of the latter can be obtained by the conjugate gradient method, which is guaranteed to converge within $(m+1)$ iterations due to $Rank(SS^T) = m$ (see Golub and Van Loan [5]). Another way of solving $(I + SS^T)d_1 = y$ is by inverting $(I + SS^T)$ directly. It is easy to show that

$$(I + SS^T)^{-1} = I - S(I + S^T S)^{-1} S^T.$$

Note that $(I + S^T S)$ is only an $m \times m$ matrix and its factorization can be obtained at minimal cost.

After d_1 and d_2 are available, d is given by

$$\begin{aligned} d &= Y_k d_1 + Z_k d_2 \\ &= \begin{pmatrix} I \\ S^T \end{pmatrix} d_1 + \begin{pmatrix} -S \\ I \end{pmatrix} d_2. \end{aligned}$$

Before going to the next iteration, we update the solution with

$$\begin{pmatrix} X_{k+1} \\ u_{k+1} \end{pmatrix} = \begin{pmatrix} X_k \\ u_k \end{pmatrix} + \alpha d,$$

and the reduced Hessian approximation with the BFGS formula

$$B_{k+1} = B_k - \frac{B_k s_k s_k^T B_k}{s_k^T B_k s_k} + \frac{y_k y_k^T}{y_k^T s_k}, \tag{2.8}$$

where y_k and s_k are given by

$$\begin{aligned} y_k &= Z_{k+1}^T [g_{k+1} - Z_k (Z_k^T Z_k)^{-1} Z_k^T g_k] \\ s_k &= (Z_{k+1}^T Z_{k+1})^{-1} Z_{k+1}^T \alpha d, \end{aligned} \tag{2.9}$$

when certain update criteria are satisfied.

In standard schemes the Lagrange multiplier is asked to satisfy

$$(Y_k^T A_k)\lambda_k = -Y_k^T g_k, \tag{2.10}$$

which is equivalent to

$$(I + SS^T)(J^T \lambda_k) = -Y_k^T g_k. \tag{2.11}$$

In our scheme, λ_k is not explicitly needed, instead only the value of $(J^T \lambda_k)$, which can be obtained by solving (2.11), has to be calculated.

To ensure convergence, a merit function is needed to monitor the progress towards the solution. The l_1 merit function is chosen for its simplicity and low computational cost, which is defined as

$$\phi_\mu(X, u) = I(X, u) + \mu \|F(X, u)\|_1.$$

Throughout this scheme, the transpose of the flow Jacobian J^T is never explicitly needed, which is desirable for many aerodynamic calculations.

3 Reduced Hessian SQP with solution refining

For the efficiency and the robustness reasons, solution refining is widely used in aerodynamic calculations. The basic idea is to get through the transient mode on cheaper, easier to solve coarse grids instead of on expensive, harder to solve fine grids. The translation of flow and design solutions from coarse grid to fine grid can be done in a variety of ways. Basic techniques include interpolation and mapping. Interesting discussions of related issues are covered by many papers including [11] and [7]. We will not go into details of them. Instead we will concentrate on the refining of the reduced Hessian matrix approximation, which has not been previously studied.

For a given number of design variables m, an interesting fact is that the size of the reduced Hessian matrix is the same (m by m) on each grid level. On grid level l, assume (1.1) is solved with X_*^l, u_*^l, Z_*^l and B_*^l. Through interpolation and mapping, an initial solution of the flow variables X_1^{l+1} and design variables u_1^{l+1} at grid level $l+1$ can be approximated. At

X_1^{l+1}, u_1^{l+1} on the new grid, the null space basis Z_1^{l+1} can be calculated. The question is how to obtain a reasonable level $l+1$ reduced Hessian approximation B_1^{l+1} at X_1^{l+1}, u_1^{l+1}. One choice is B_*^l. However, B_*^l is intended to approximate the reduced Hessian $Z_*^{l\,T} H_*^l Z_*^l$, while B_1^{l+1} is intended to approximate the reduced Hessian $Z_1^{l+1\,T} H_1^{l+1} Z_1^{l+1}$. Since the Z matrices are not normalized, there is a potential mismatch of information between the two reduced Hessian approximations. A better choice is to treat the reduced Hessian in a normalized null space as invariant, which leads to

$$\begin{aligned} & (Z_1^{l+1}(Z_1^{l+1\,T} Z_1^{l+1})^{-1/2})^T H_1^{l+l}(Z_1^{l+1}(Z_1^{l+1\,T} Z_1^{l+1})^{-1/2}) \\ \approx\ & (Z_*^l(Z_*^{l\,T} Z_*^l)^{-1/2})^T H_*^l(Z_*^l(Z_*^{l\,T} Z_*^l)^{-1/2}), \end{aligned}$$

which in turn implies

$$\begin{aligned} & Z_1^{l+1\,T} H_1^{l+1} Z_1^{l+1} \\ \approx\ & (Z_1^{l+1\,T} Z_1^{l+1})^{1/2}(Z_*^{l\,T} Z_*^l)^{-1/2} Z_*^{l\,T} H_*^l Z_*^l \\ & (Z_*^{l\,T} Z_*^l)^{-1/2}(Z_1^{l+1\,T} Z_1^{l+1})^{1/2}. \end{aligned}$$

Hence it is reasonable to choose

$$B_1^{l+1} = (Z_1^{l+1\,T} Z_1^{l+1})^{1/2}(Z_*^{l\,T} Z_*^l)^{-1/2} B_*^l (Z_*^{l\,T} Z_*^l)^{-1/2}(Z_1^{l+1\,T} Z_1^{l+1})^{1/2}.$$

Since in our case a Z matrix always has full rank, $Z^T Z$ is always positive definite, and from its eigen-decomposition $(Z^T Z)^{-1/2}$, as well as $(Z^T Z)^{1/2}$, can be obtained. Since the number of design variables m is much less than the number of flow variables n, the computation of the eigen-decomposition of $Z^T Z$, which is of size $m \times m$, is not significant and is affordable for many applications. In addition, since the decomposition is only carried out once at each grid level, the extra cost introduced by the Hessian refining is likely to be minimal.

4 Quasi-one-dimensional Euler equations

For our purposes here, we have chosen one popular form of central finite differences with nonlinear artificial dissipation,

The quasi-1D Euler equations are

$$\mathbf{F}(\mathbf{Q}) = \partial_x \mathbf{E}(\mathbf{Q}) + \mathbf{H}(\mathbf{Q}) + \mathbf{D}(\mathbf{Q}) = 0 \quad 0.0 \le x \le 1.0 \tag{4.1}$$

where

$$\mathbf{Q} = \begin{bmatrix} \rho \\ \rho u \\ e \end{bmatrix}, \quad \mathbf{E} = a(x) \begin{bmatrix} \rho u \\ \rho u^2 + p \\ u(e+p) \end{bmatrix}, \quad \mathbf{H} = \begin{bmatrix} 0 \\ -p\partial_x a(x) \\ 0 \end{bmatrix} \tag{4.2}$$

with ρ (density), u (velocity), e (energy), $p = (\gamma - 1)(e - 0.5\rho u^2)$ (pressure), $\gamma = 1.4$ (ratio of specific heats), and $a(x) = (1. - 4.(1 - a_t)x(1 - x))$ (the nozzle area ratio), with $a_t = 0.8$. For a given area ratio and shock location (here $x = 0.7$) an exact solution can be obtained from the method of characteristics.

We choose one popular form of central finite differences to discretize these equations.

$$\begin{aligned} \partial_x q \approx \delta_x q_j = \frac{q_{j+1} - q_{j-1}}{2\Delta x} \quad & j = 1, \ldots, Jmax \\ \Delta x = 1.0/(Jmax - 1), \quad & u_j = u(j\Delta x) \end{aligned} \tag{4.3}$$

It is common practice and well known that artificial dissipation must be added to the discrete central difference approximations in the absence of any other dissipative mechanism, especially for transonic flows, see Pulliam[8].

For simplicity here, we use a constant coefficient dissipation of the form

$$D^4(\mathbf{Q}) = \nabla_x \left(\epsilon_j^{(4)} \Delta_x \nabla_x \Delta_x \mathbf{Q}_j \right) \tag{4.4}$$

with

$$\nabla_\xi q_j \;\; = \;\; q_j - q_{j-1}, \quad \Delta_\xi q_j = q_{j+1} - q_j \tag{4.5}$$

with a typical value of $\epsilon^{(4)} = \frac{1}{100}$.

Boundary condition at $j = 1$ and $j = Jmax$ are defined in terms of physical conditions (taken from exact solution values) and will be treated as Dirchlet (fixed conditions) for now.

The total system we shall solve is

$$\mathcal{F}(\mathbf{Q}) = \begin{cases} \delta_x \mathbf{E}(\mathbf{Q})_j - \mathbf{H}(\mathbf{Q})_j + D_j^4(\mathbf{Q}), & j = 1, \cdots, J_N \\ B(\mathbf{Q})_i = 0, & i = 0, J_N \end{cases} \tag{4.6}$$

5 Test results for a nozzle design problem

The nozzle design problem. We assume that a target velocity distribution u_j^*, is given for each computational grid point. The design problem we are trying to solve is

> *Find y_i, $i = 1, \cdots, m$ (spline coefficients describing $a(x)$), such that $\frac{1}{2}\sum_{j=1}^{Jmax}(u_j - u_j^*)^2$ is minimized subject to (4.6) being satisfied.*

For our test examples, the breakpoints of the spline are evenly distributed in the interval $[0, 1]$.

Some implementation issues. At each grid level l, the design problem is solved using the reduced Hessian SQP to a specified tolerance ϵ^l (in our testing, ϵ is uniformly set to $1.E-7$), then grid is refined and the initial estimates to the design variables, flow variables, as well as the reduced Hessian on grid $l + 1$ are obtained from corresponding solutions on grid l. This procedure is repeated until the solution on the desired grid level is reached.

For our tests, a flat nozzle shape and a flat flow are used as starting data on grid 1. The starting reduced Hessian approximation is $B_0^1 = {Z_0^1}^T Z_0^1$.

Design results with grid size 65 and 7 design variables. In order to assess the efficiency of solution refining, we first choose to solve the design problem with grid size 65 and 7 spline coefficients. This is quite a difficult problem because of over parameterization. We use the cost of solving the flow equations (without the presence of design variables) as a baseline to compare the cost of the reduced Hessian SQP with and without solution refining.

Figure 1 shows 2 level flow solutions against the target solution. It also shows the convergence history of the flow residuals. The flow problem is first solved with grid size 33 (upper subgraph). A significant number of iterations were taken due to difficulties in the transient regime (upper right). Then the solution is refined with grid size 65 (lower left). Due to good initial guess from the coarse grid solution, only 5 iterations were required to reach the tight tolerance (lower right).

Figure 2 shows the design result of the reduced Hessian SQP without solution refining. Although the convergence of flow residuals and projected gradients appears to be superliner, it took a fair amount of iterations to get through the transient regime. The target, initial and final solutions are marked with solid, dashed and checked solid lines, respectively. The reductions in the projected gradient and the flow residual are marked with $+$ and $*$, respectively. These notions are used consistently throughout the rest of this paper.

Figures 3 and 4 show the test results of the reduced Hessian SQP with two levels of refining. First the design is solved on grid level 1 with grid size 33 (Figure 3). Then it is subsequently solved on grid level 2 with the desired grid size 65 starting from the grid level 1 solution (Figure 4). Due to the good initial information supplied from coarse grids, it only took 10 (versus 35 without solution refining) expensive fine grid iteration to reach the tolerance. The overall saving over no solution refining in flop counts is about 33%. The final cost is only about 3 times as much as the cost of a single flow solution run.

The test results are summarized in Table 1.

Num. of Dsgn. Vars.	Grid Levels	Total Flops	Num. of Iters.	Cost Ratio
0	2	2709573	30(1)+5(2)	1.000
7	0	13631377	35	5.03
7	2	9166365	26(1)+10(2)	3.38

Table 1: Efficiency of solution refining (grid size 65)

Design results with grid size 513 and 15 design variables. To make the design problem more challenging, we next solve the problem with grid size 513 and 15 design variables. This time the reduced Hessian SQP without solution refining failed to solve the problem (stuck in the transient regime), while the scheme with solution refining solved the problem successfully.

Five levels of grid refining were carried out. Solutions on these five grid levels are shown in Figures 5 to 9. The results are summarized in Table 2. As expected, a relatively large

number of iterations were performed on grid 1 for getting through the transient regime (Figure 5). As the grid is refined, the convergence is getting smoother (Figures 6 to 9). On the final grid it only took 12 iterations to converge to the tight tolerance.

Grid Level	1	2	3	4	5
Flops Count	17570765	15228630	22709106	38298903	75681269
Iterations	39	18	14	12	12
Grid Size	33	65	129	257	513

Table 2: Results summary for grid size 257 and 15 design variables with solution refining.

Testing with a various number of design variables and various grid sizes. Finally, we give the full set of the test results. The reduced Hessian SQP scheme with solution refining is tested on the nozzle design problem using a various number of design variables, i.e., $0, 1, 3, 7, 15$ and various grid sizes, i.e., $33, 65, 129, 257, 513$. We want to point it out that each grid is associated with three flow variables. Hence the number of total flow variables is $99, 195, 387, 771, 1539$ (3 times each grid size), respectively. Table 3 summarizes the test results, which is visualized in Figure 10.

The problem with grid size 33 is solved with no solution refining, while the problem with grid size 65 is solved with 2 levels of solution refining, the problem with grid size 129 is solved with 3 levels of solution refining, and so on and so forth.

For each grid size, the cost with no design variables is used as a basis to measure the costs with a various number design variables.

It seems that the cost of solving the design problem is about the same as or only one order of magnitude more than the cost of calculating the nonlinear flow, which is very promising for aerodynamic design optimization. Figure 10 shows that on the one hand, as the grid size increases, the relative cost of the design calculation is increased linearly. On the other hand it shows that as the number of design variables increases, the cost of design calculation appears to increase faster than linearly. We feel that this is caused by over-parameterization that results in much hard problems as more and more design variables are introduced for the same design problem. We believe that the increase should be linear without excessive over-parameterization.

6 Concluding remarks

This paper shows that solution refining can be combined with the reduced Hessian SQP scheme for aerodynamic design optimization. A particular useful technique introduced in this paper is the reduced Hessian refining under a variable metric formula. Test results show that the efficiency and the robustness of the reduced Hessian SQP scheme are significantly improved through solution refining. We believe that the efficiency could be further improved for certain problems through refining in the design variable space by gradually increasing the number of variables, particularly for problems with a significant number of design variables.

This brings forth a more challenging research topic for the efficient and effective reduced Hessian refining. Finally, applications of the reduced Hessian SQP scheme to 2D and 3D problems are currently under investigation by the authors.

References

[1] D. FENG AND T. H. PULLIAM, *An all-at-once reduced Hessian sqp scheme for aerodynamic design optimization*, Tech. Rep. 95.19, Research Institute for Advanced Computer Science, NASA Ames Research Center, Moffett Field, California, 1995.

[2] R. FLETCHER, *Practical Methods of Optimization, Second Edition*, John Wiley & Sons, second ed., 1989.

[3] D. GABAY, *Reduced quasi-Newton methods with feasibility improvement for nonlinearly constrained optimization*, Mathematical Programming Studies, 16 (1982), pp. 18–44.

[4] J. C. GILBERT, *Maintaining the positive definiteness of the matrices in reduced Hessian methods for equality constrained optimization*, Math. Programming, 50 (1991), pp. 1–28.

[5] G. H. GOLUB AND C. F. V. LOAN, *Matrix Computations*, The John Hopkins University Press, second ed., 1989.

[6] A. JAMESON, *Aerodynamic design via control theory*, Journal of Scientific Computing, 3 (1988), pp. 233–260.

[7] G. KURUVILA, S. TA'ASAN, AND M. D. SALAS, *Airfoil design and optimization by the one-shot method*, AIAA Paper 95-0478, (1995).

[8] T. PULLIAM, *Artificial dissipation models for the Euler equations*, AIAA Paper 85-0438, (1985).

[9] J. REUTHER, S. E. CLIFF, R. M. HICKS, AND C. P. VAN DAM, *Practical design optimization of wing/body configuration using the Euler equations.* AIAA paper 92-2633, 1992.

[10] Y. XIE AND R. H. BYRD, *Practical update criteria for reduced Hessian SQP, Part I: Global analysis*, Tech. Rep. CU-CS-753-94, Computer Science Department, University of Colorado, Boulder, 1994.

[11] D. P. YOUNG, W. P. HUFFMAN, M. B. BIETERMAN, R. G. MELVIN, F. T. JOHNSON, C. L. HILMES, AND A. R. DUSTO, *Issues in design optimization methodology*, Tech. Rep. BCSTECH-94-007 REV. 1, Boeing Computer Services, Seattle, Washington, 1994.

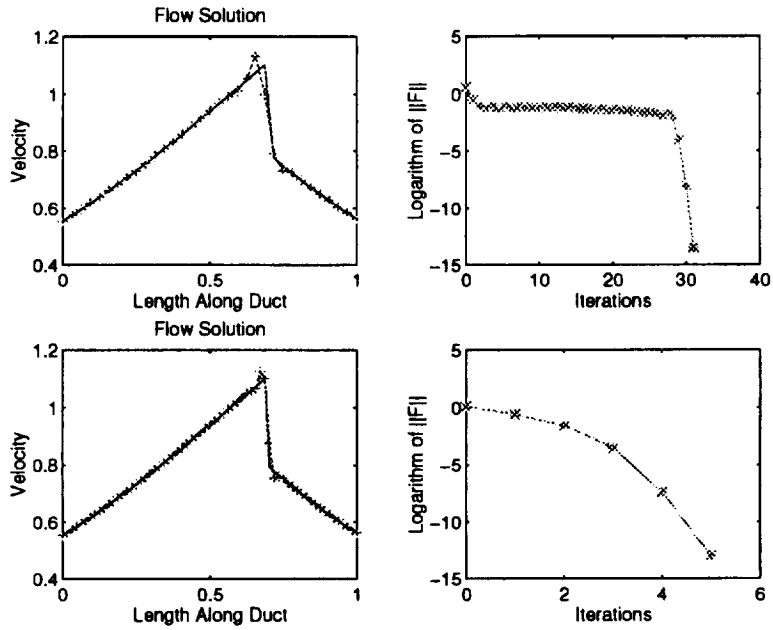

Figure 1: Flow solutions with 2 levels of solution refining. Grid size = 33, 65.

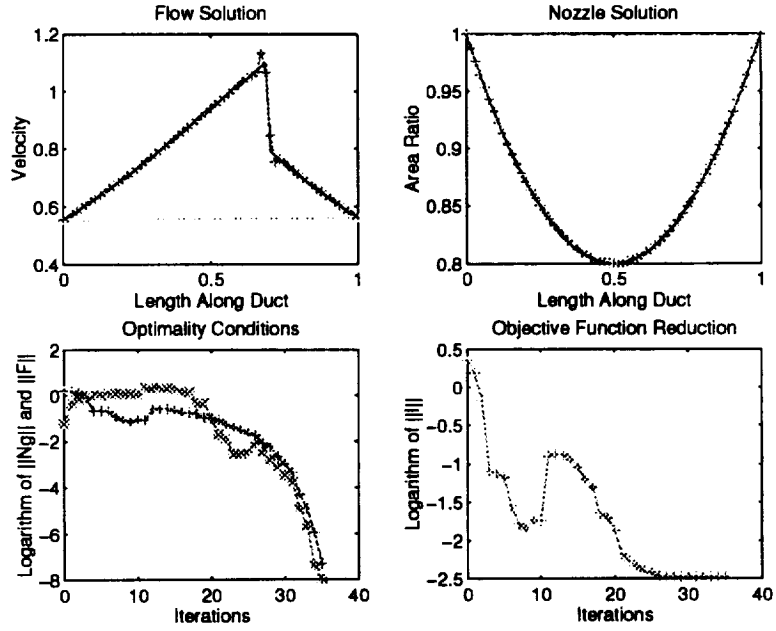

Figure 2: Design solutions without solution refining. 7 design variables and grid size = 65.

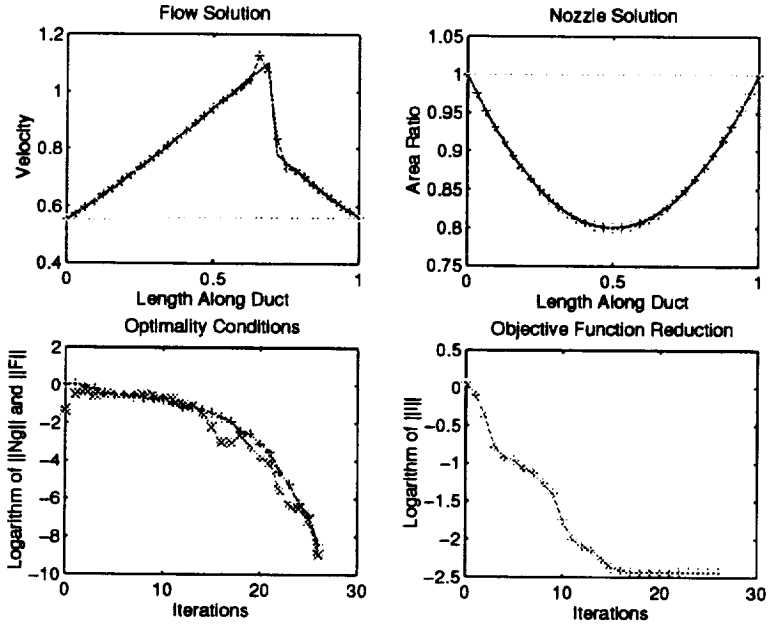

Figure 3: Design solutions on grid 1 with 7 design variables and grid size = 33.

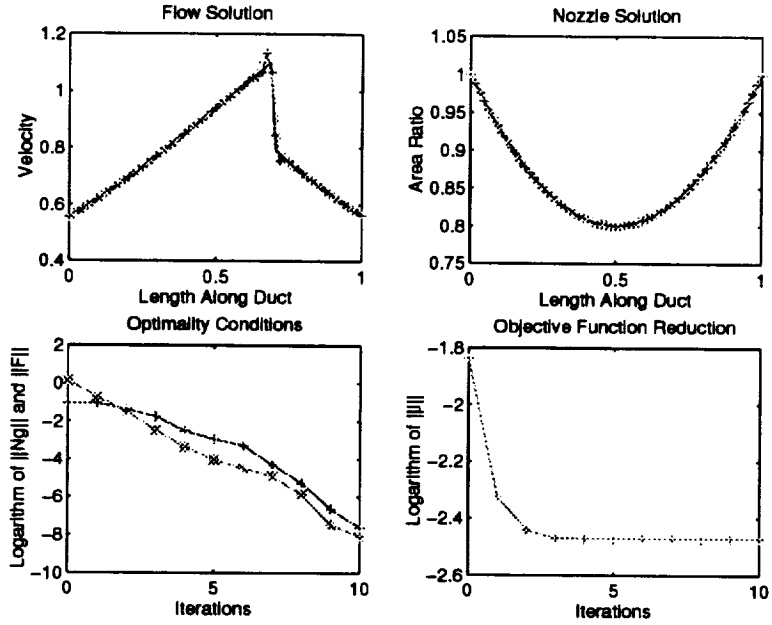

Figure 4: Design solutions on grid 2 with 7 design variables and grid size = 65.

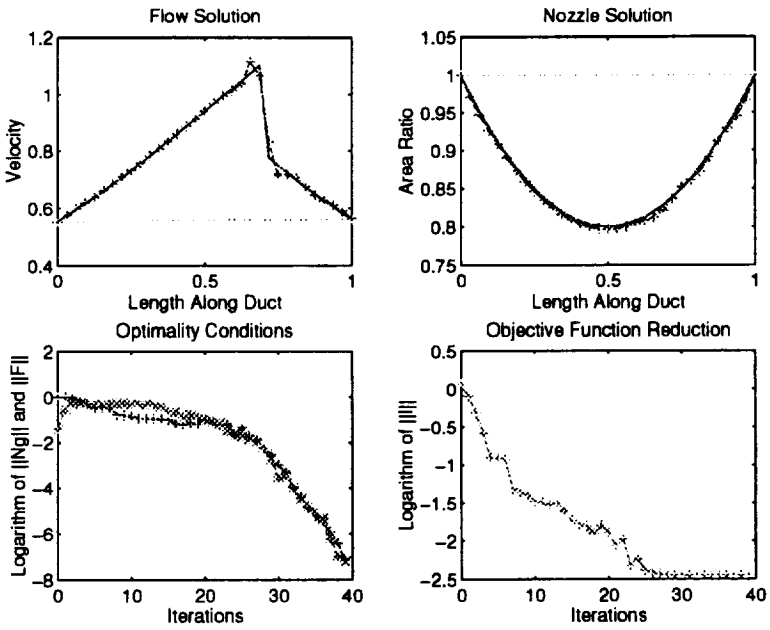

Figure 5: Design solutions on grid 1 with 15 design variables and grid size = 33

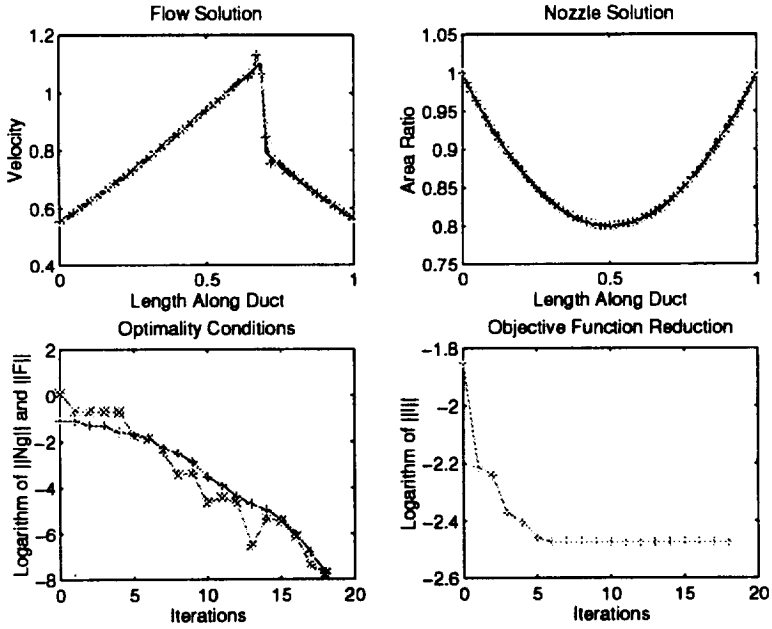

Figure 6: Design solutions on grid 2 with 15 design variables and grid size = 65.

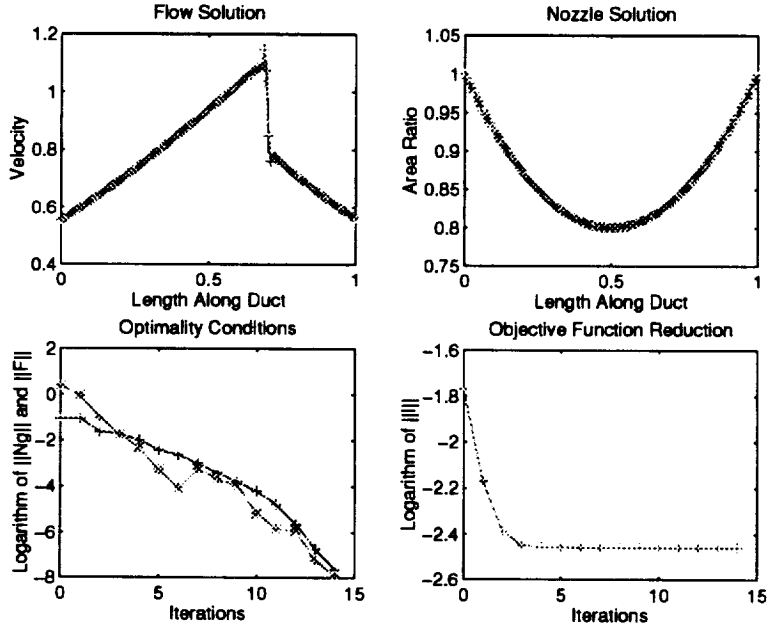

Figure 7: Design solutions on grid 3 with 15 design variables and grid size = 129.

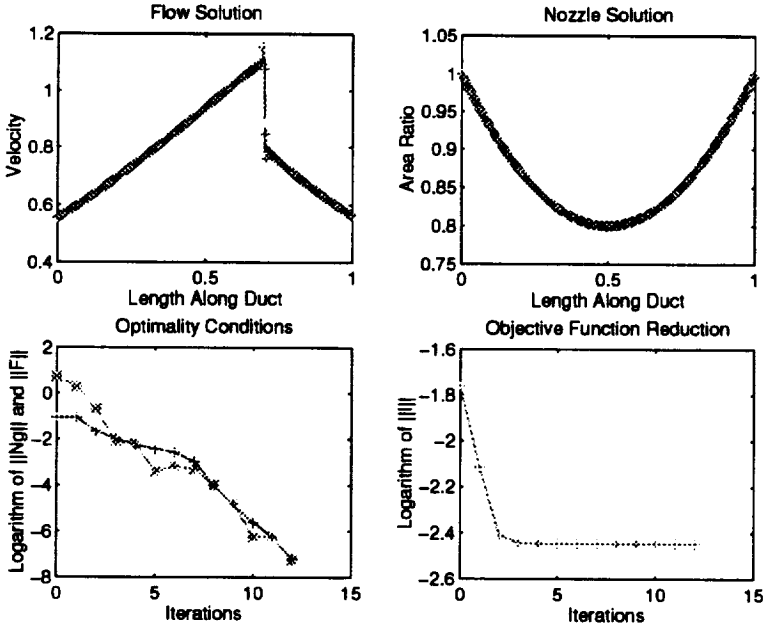

Figure 8: Design solutions on grid 4 with 15 design variables and grid size = 257.

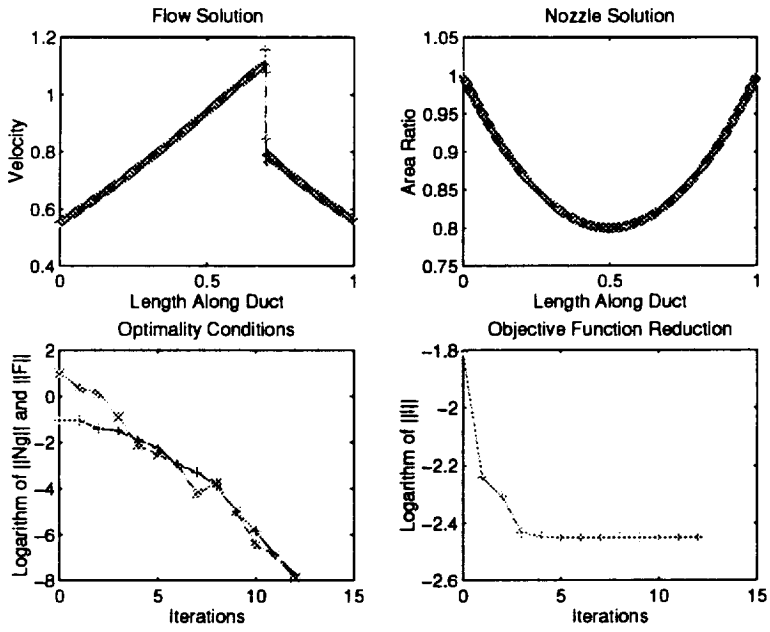

Figure 9: Design solutions on grid 5 with 15 design variables and grid size = 513.

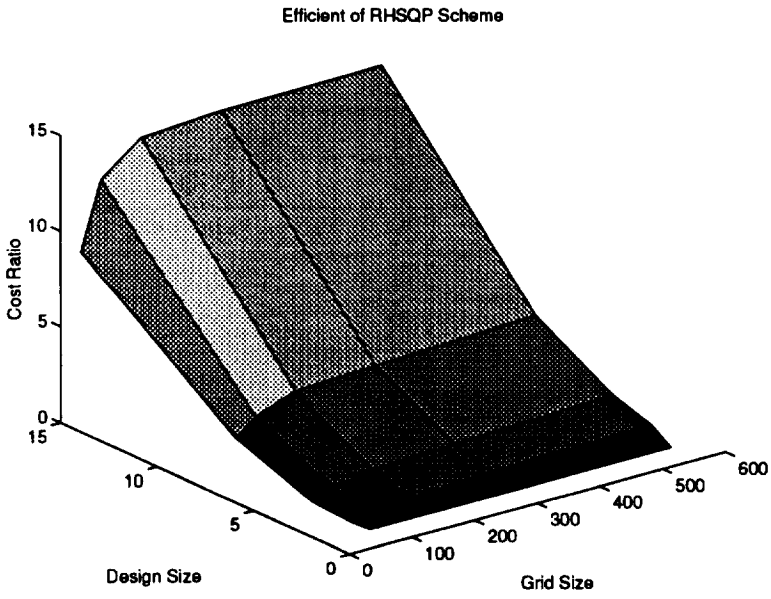

Figure 10: Efficiency of reduced Hessian SQP scheme.

Num. of Des. Vars.	Grid Size	Flops	Cost Ratio
0	33	2036491	1.00
0	65	2709573	1.00
0	129	4040497	1.00
0	257	6687365	1.00
0	513	11965583	1.00
1	33	1897820	0.94
1	65	3227728	1.20
1	129	5559882	1.38
1	257	10195908	1.53
1	513	20611283	1.73
3	33	2181578	1.08
3	65	4054968	1.50
3	129	7315226	1.82
3	257	13771675	2.06
3	513	28251307	2.37
7	33	5237019	2.58
7	65	9166365	3.38
7	129	16794298	4.16
7	257	29052365	4.35
7	513	56129543	4.70
15	33	17570765	8.64
15	65	32799395	12.11
15	129	55508501	13.74
15	257	93807404	14.03
15	513	169488673	14.17

Table 3: Efficiency of the all-at-once scheme

RIACS
Mail Stop T041-5
NASA Ames Research Center
Moffett Field, CA 94035